Available online at www.sciencedirect.com
SCIENCE DIRECT®

ELSEVIER

Polymer 47 (2006) 3302–3314

polymer

www.elsevier.com/locate/polymer

Copolymerization of ethene with norbornene using palladium(II) α-diimine catalysts: Influence of feed composition, polymerization temperature, and ligand structure on copolymer properties and microstructure

Jens Kiesewetter, Burçak Arikan, Walter Kaminsky *

Institute of Technical and Macromolecular Chemistry, University of Hamburg, Bundesstrasse 45, D-20146 Hamburg, Germany

Received 30 November 2005; received in revised form 14 February 2006; accepted 5 March 2006
Available online 3 April 2006

Abstract

Four cationic palladium(II) α-diimine complexes, [{ArN=C(R)–C(R)=NAr}Pd(Me)(CH$_3$CN)]BAr$^f_4$ (**1**, R = H, Ar = 2,6-Me$_2$C$_6$H$_3$, BAr$^f_4$ = B[3,5-C$_6$H$_3$(CF$_3$)$_2$]$_4$; **2**, R = CH$_3$, Ar = 2,6-*i*Pr$_2$C$_6$H$_3$; **3**, R = CH$_3$, Ar = 2-*t*BuC$_6$H$_4$; **4**, R,R = An, Ar = 2,6-*i*Pr$_2$C$_6$H$_3$) were used for the copolymerization of ethene with norbornene. The copolymerization behavior of the catalysts and the influence of the polymerization temperature were investigated. The copolymers were characterized using ^{13}C NMR spectroscopy, differential scanning calorimetry, and gel permeation chromatography techniques. Sterically demanding *ortho -N*-aryl substituents and rigid bulky bridge units increase the copolymer molar masses, while the incorporation level of norbornene is decreased. Microstructures with isolated norbornene units and alternating sequences are predominant. Less bulky substituted catalysts yield copolymers with higher norbornene contents and lower molar masses. Norbornene diblock sequences are dominant which are exclusively *racemic* connected, indicating that the insertion proceeds under chain end control. Optimal polymerization results are achieved at temperatures between 10 and 30 °C, while temperatures below 0 °C result in lower polymerization rates and molar masses. Above 30 °C, activities, molar masses, and norbornene incorporation decreases due to catalyst decomposition.

Keywords: Ethene/norbornene copolymers; Late transition metal catalysts; Microstructure

1. Introduction

Copolymers of ethene and norbornene (cyclic olefin copolymers, COCs) are amorphous thermoplastics of high commercial and academic interest. The combination of properties like high transparency, glass transition temperature, and refractive index, together with an excellent processability, makes them an alternative for materials like polycarbonate and polymethyl methacrylate in the field of optical components and high capacity DVDs and CDs [1,2]. Due to their very low vapor permeability, excellent bio compatibility, and high resistance against acids, bases, and aliphatic organic solvents these polymers are also valuable materials for packing, blister foils, and medical equipment.

Heterogeneous Ti and V catalysts were developed to homo- and copolymerize norbornene shortly after the discovery of the Ziegler–Natta catalysts in the 1950s [3–6], but these catalysts possessed many disadvantages like low activity and varying product qualities. The breakthrough was achieved by our workgroup in the end of the 1980s with the development of homogeneous metallocene/methylaluminoxane (MAO) catalyst systems for the copolymerization of ethene and norbornene [7–10]. With these catalytic systems, it is possible to influence the product properties by choice of the ligand framework and the appropriate polymerization conditions. Eventually, this led to the commercial TOPAS product line of COC materials by Ticona.

Catalytic systems based on early transition metals are very sensitive to polar impurities and oxygen containing groups in the monomer. Due to their less electrophilic behavior and lower oxidation state, catalysts based on late transition metals like Ni and Pd show a higher tolerance to polar impurities. However, late transition metal complexes were not supposed to produce high molecular weight polymers, since late transition metal alkyl complexes show a strong tendency to undergo β-hydride elimination reactions. Therefore, the first application of late transition metal complexes was in the field of ethene oligomerization in the Shell higher olefin process (SHOP) developed by Keim et al. in the early 1970s [11–13]. In this

---

* Corresponding author. Tel.: +49 40 42838 3162; fax: +49 40 42838 6008.
E-mail address: kaminsky@chemie.uni-hamburg.de (W. Kaminsky).

0032-3861/$ - see front matter © 2006 Elsevier Ltd. All rights reserved.
doi:10.1016/j.polymer.2006.03.020

process, square planar Ni complexes with anionic P^O chelate ligands were applied. Although these catalysts were later tuned to give high molar mass products [14–17], a breakthrough was achieved with the discovery by Brookhart et al. [18–20] that cationic Ni and Pd complexes with bulky aryl-substituted α-diimine ligands are very efficient catalysts for the polymerization of ethene and α-olefins.[1] These catalysts are less sensitive to polar impurities and functional groups [26–28] and even allow the suspension polymerization of ethene in aqueous media [29–33].

In 1998, Goodall et al. reported in two patents about the ethene/cycloolefin copolymerization with a variety of late transition metal catalysts [34,35]. Among these were bulky aryl substituted α-diimine complexes with Pd as the metal center. We recently reported about the influence of the sterical bulk of the α-diimine substituents on the copolymerization of ethene and norbornene in a screening-like procedure [36]. On basis of these results, we investigated the properties of four well-defined palladium α-diimine catalysts concerning the copolymerization of ethene and norbornene. The catalysts were synthesized as discrete, polymerization active species. The influence of the monomer ratio and the polymerization temperature on the resulting copolymers was investigated.[2] In addition, the copolymer microstructure was determined by ^{13}C NMR techniques.

2. Experimental section

2.1. General

All manipulations were performed using standard Schlenk, syringe, and drybox techniques unless otherwise noted. Argon was purchased from Linde and purified by passage through a Messer Oxisorp cartridge. Solid organometallic compounds were stored and transferred in an argon filled drybox. Ethene (Linde) and toluene were purified by passage through columns with BASF R3-11 catalyst and 3 Å molecular sieve. Norbornene (Acros) was stirred for 48 h with triisobutylaluminum at 50 °C and distilled off. A solution in toluene of 6–7 mol/l was used for polymerizations.

Chemicals for ligand syntheses were purchased from Merck, Fluka, and Aldrich. Syntheses were performed according to literature procedures [21–25]. Dichloro(1,5-cyclooctadiene)palladium(II) was purchased from ABCR. Syntheses of (1,5-cyclooctadiene)chloromethylpalladium(II) [37], sodium {tetrakis[3,5-bis(trifluoromethyl)-phenyl]borate} ($Na[BAr^f_4]$) [38], $\{[ArN{=}C(H)–C(H){=}NAr]PdMe(CH_3CN)\}BAr^f_4$ ($Ar = 2,6\text{-}Me_2C_6H_3$) [19], $\{[ArN{=}C(CH_3)–C(CH_3){=}NAr]PdMe(CH_3CN)\}BAr^f_4$ ($Ar = 2,6\text{-}(iPr)_2C_6H_3$) [19], $\{[ArN{=}C(CH_3)–C(CH_3){=}NAr]PdMe(CH_3CN)\}BAr^f_4$ ($Ar = 2\text{-}tBuC_6H_4$) [39], and $\{[ArN{=}C(An)–C(An){=}NAr]PdMe(CH_3CN)\}BAr^f_4$ ($Ar = 2,6\text{-}(iPr)_2C_6H_3$) [27] were performed according to literature procedures. Catalyst solutions in fluorobenzene were freshly prepared, stored at −28 °C, and used within 2–3 days since slow decomposition was observed resulting in the formation of Pd^0.

2.2. Characterization

^{1}H and ^{13}C NMR spectra were recorded on a Bruker Avance 400 Ultrashield spectrometer. Spectra of organometallic compounds were recorded at 400.15 MHz and room temperature. Polymer samples were measured at 100.62 MHz and 100 °C using 200 mg of polymer in 2.3 ml of 1,2,4-trichorobenzene and 0.5 ml of 1,1,2,2-tetrachloroethane-d_2. Chemical shifts are reported relative to residual $CHCl_3$ (δ 7.24 ppm for ^{1}H) and to $C_2D_2Cl_4$ (δ 74.24 ppm for ^{13}C). Differential scanning calorimetry curves were recorded on a Mettler Toledo DSC 821^e instrument calibrated with *n*-heptane ($T_m = -90.6$ °C), mercury ($T_m = -38.8$ °C), gallium ($T_m = 29.8$ °C), indium ($T_m = 156.6$ °C), and zinc ($T_m = 419.5$ °C). Results of the second thermal cycle are presented exclusively. High-temperature gel permeation chromatography (GPC) measurements were performed in 1,2,4-trichlorobenzene at 140 °C using a Waters GPCV 2000 instrument with HT 10^6, 10^4, and 10^3 Å columns. The instrument operated with a combined refractive index and viscosity detector unit, which allowed the calculation of appropriate Mark–Houwink constants for every single polymer. Calibration was applied using polystyrene standards (PSS).

2.3. General polymerization procedure

Norbornene homopolymerization runs were performed in a 200 ml glass reactor equipped with a heat jacket and a magnetic stirrer. All other polymerization runs were performed in a Büchi BEP 280 laboratory autoclave with a type I glass pressure vessel, which allowed ethene pressures up to 6 bar. Temperature was adjusted with a heat jacket connected to a thermostat allowing adjustment of the polymerization temperature with an accuracy of ±0.5 °C. During the polymerization runs, the ethene pressure was kept constant using a pressure control. The ethene consumption was monitored with a Brooks 5850 TR mass flow meter and a Westphal WMR 4000 control unit. For a typical polymerization experiment, the reactor was evacuated at 90 °C for 1 h and then cooled down to the desired temperature. Subsequently, the reactor was charged with norbornene, toluene, and ethene up to a volume of 200 or 400 ml at the desired feed composition. The polymerization was started by injection of the catalyst solution. The reaction was quenched by addition of 5 ml ethanol.

All polymer solutions were stirred overnight with 100 ml of diluted hydrochloric acid. After phase separation, the organic phase was washed three times with water and reduced to 50–70 ml at the rotary evaporator. The polymer was precipitated with a 10-fold excess of ethanol, filtered off, washed with ethanol, and dried in vacuum at 60 °C until the weight remained constant.

---

[1] Ni and Pd α-diimine complexes have been intensively investigated before [21–25].

[2] The catalysts **1** and **2** have already been described by us with regard to the influence of the monomer ratio on activity, norbornene incorporation, and thermal behavior of the polymer [36]. In order to achieve a better comparison with the other catalysts, the results are given here as well.

3. Results and discussion

The catalysts investigated in this study are shown in Fig. 1. Catalyst **1** carries small methyl group substituents in ortho position of the *N*-aryl system and has a non-substituted ethane diimine bridge unit. This should allow easy coordination of bulky monomers like norbornene and lead to high incorporation levels. The catalysts **2** and **4** carry bulky isopropyl *ortho*-substituents and bulky 2,3-butane diimine or acenaphthene diimine bridge units, respectively. Therefore, the incorporation level should be lower due to the complicated monomer coordination. Catalyst **3** carries only one ortho substituent leading to two possible isomers with a cis and trans conformation of the bulky *tert*-butyl groups. These isomers should show different copolymerization behavior.

3.1. Copolymerizations at different monomer ratios

While ethene is supplied continuously via a pressure control, norbornene is consumed during the course of the reaction. In order to remain a constant comonomer ratio, the norbornene turnover has to be kept low, preferably under 10%. With common early transition metal catalysts like metallocenes this is comparatively facile since norbornene-rich feed compositions are necessary to achieve higher norbornene incorporation [40,41]. However, catalysts with Pd(II) as the metal center show very high incorporation levels even at low norbornene fractions in the feed [36]. The chosen polymerization conditions were a compromise between low norbornene turnover and yielding sufficient product for full characterization. Table 1 summarizes the polymerization conditions and results of the experiments at different comonomer ratios in the feed are summarized in the Tables 1–4.

3.1.1. Norbornene incorporation

The level of norbornene incorporation as well as the distribution along the polymer chain and the stereochemical orientation is of vital importance for the macroscopic properties of the polymers. The most powerful method to determine the norbornene incorporation and the microstructure of the polymer is ^{13}C NMR spectroscopy. Today it is widely accepted that norbornene is inserted in an 2,3-*cis*-*exo* orientation [7]. The spectra are of high complexity due to the large number of different monomer sequences including norbornene microblocks of variable lengths. The number of resonances is further enhanced by the possible stereochemical orientation of norbornene units in microblocks and alternating structures. However, an assignment of signal groups to individual carbon atoms of the norbornene and ethene unit is comparatively straightforward [7,42]. By this means, the norbornene content of polymers produced by metallocene/MAO catalysts can be calculated. The method has to be slightly modified if late transition metal catalysts are used and is described in a previous paper [36]. Fig. 2 shows the mole fraction of

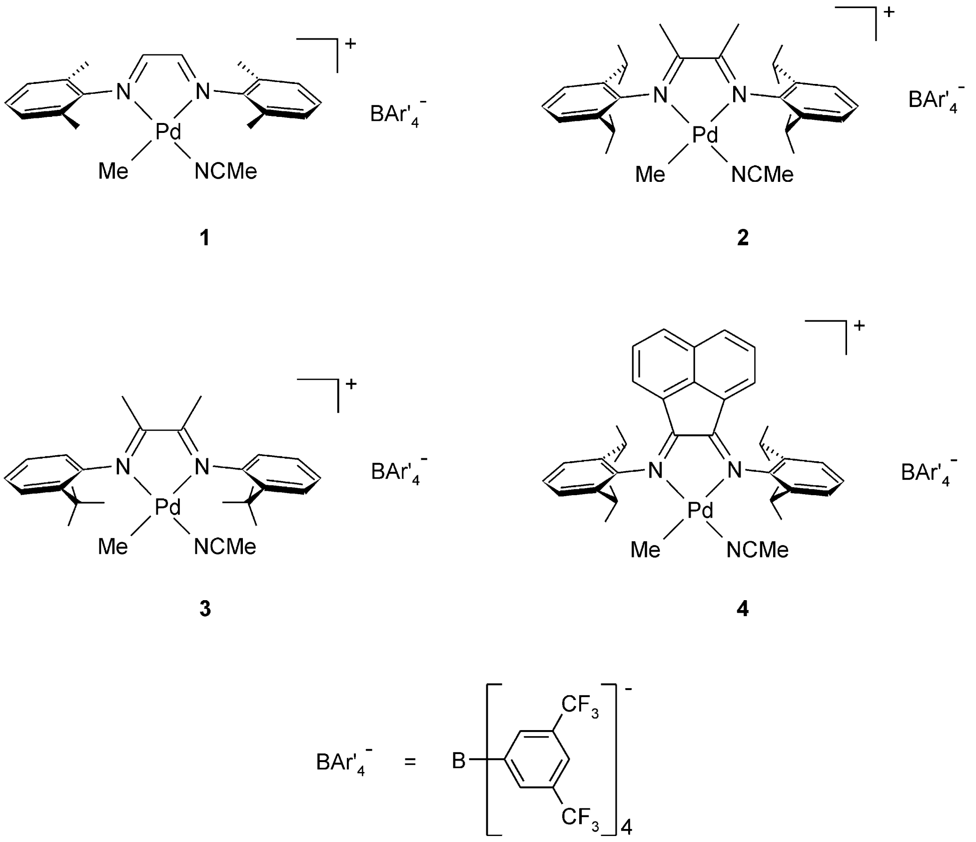

Fig. 1. Pd(II) α-diimine complexes investigated for the copolymerization of ethene and norbornene.

Table 1
Copolymerization of ethene and norbornene at different comonomer ratios using catalyst **1**

Conditions[a]				Results			
x_N[b] (°C)	c_{mon}[c] (mol l^{-1})	n_{Pd} (μmol)	t_{pol} (h)	Activity[d]	T_g (°C)	M_w (g mol^{-1})	M_w/M_n
0.00	0.70	16.76	1.0	36	−75	1500	1.4
0.05	0.76	4.19	1.0	161	98	24,000	1.4
0.10	0.80	4.19	1.0	243	126	39,000	2.0
0.20	0.71	4.19	1.0	120	146	59,000	1.8
0.34	0.71	8.38	1.0	67	169	66,000	1.8
0.40	0.70	16.76	1.0	57	177	60,000	1.8
0.50	0.70	16.76	1.0	50	189	62,000	1.9
0.59	0.70	16.76	1.0	34	216	54,000	1.6
0.80	0.70	16.76	2.0	11	[e]	40,000	1.7
0.90	0.70	33.54	2.0	10	[e]	20,000	2.9[f]
1.00	0.90	33.54	72.0	<1	[e]	[g]	[g]

Results of polymerizations at 30 °C in toluene.

[a] Total reaction volume 200 ml (norbornene homopolymerization: 150 ml).

[b] Mole fraction of norbornene in the feed.

[c] Total monomer concentration.

[d] Activity: kg_{pol} mol_{Pd}^{-1} h^{-1}.

[e] Polymer bi- or multimodal. Polymer decomposes.

[f] Polymer bi- or multimodal.

[g] Polymer insoluble in 1,2,4-trichlorobenzene.

norbornene in the polymer as a function of the mole fraction of norbornene in the feed (copolymerization diagram).

The four catalysts cover a wide range of norbornene incorporation levels. It is possible to formulate a relation between the steric demand of the ligand and the achievable norbornene incorporation. Catalyst **1**, bearing small methyl groups in ortho position of the *N*-aryl system and an unsubstituted ethane diimine bridge unit, has the least blocked coordination site. Therefore, norbornene coordination and insertion is comparatively facile. The incorporation of norbornene is almost independent of the feed composition if x_N exceeds 0.20 and does not surpass $X_N = 0.62$.

The bulky isopropyl *ortho*-substituents of catalyst **2** and **4** hinder the coordination of the norbornene. The incorporation level is much lower though still higher than with most of the early transition metal catalysts. At norbornene poor conditions both catalysts show the behavior of an almost ideal copolymerization, i.e. the norbornene incorporation reflects the feed composition. The higher steric demand of the butane diimine bridge of catalyst **2** compared to the aromatic acenaphthene diimine bridge of **4**, leads to an even lower norbornene incorporation. Catalyst **3** carries only one bulky substituent in ortho position of the *N*-aryl system. The relatively open structure of the coordination site allows facile norbornene coordination and insertion. The incorporation level lies between those of catalysts with methyl and isopropyl *ortho*- *N*-aryl substituents.

Table 2
Copolymerization of ethene and norbornene at different comonomer ratios using catalyst **2**

Conditions[a]				Results			
x_N[b] (°C)	c_{mon}[c] (mol l^{-1})	n_{Pd} (μmol)	t_{pol} (h)	Activity[d]	T_g (°C)	M_w (g mol^{-1})	M_w/M_n
0.00	0.69	7.77	1.0	185	−67	142,000	2.0
0.10	0.70	7.77	1.0	75	−28	134,000	1.9
0.20	0.70	7.77	1.0	63	10	123,000	1.8
0.34	0.71	7.77	1.0	53	48	106,000	1.7
0.40	0.70	7.77	1.0	57	63	101,000	1.8
0.50	0.71	7.82	1.0	48	82	820,00	1.5
0.60	0.70	7.82	1.0	37	97	490,00	1.8
0.81	0.87	7.82	2.0	8	120	170,00	1.9
0.90	1.69	26.22	2.0	4	[e]	190,00	2.0[f]
1.00	0.75	15.65	72.0	<1	[e]	[g]	[g]

Results of polymerizations at 30 °C in toluene.

[a] Total reaction volume 200 ml (norbornene homopolymerization: 188 ml).

[b] Mole fraction of norbornene in the feed.

[c] Total monomer concentration..

[d] Activity: kg_{pol} mol_{Pd}^{-1} h^{-1}.

[e] Polymer bi- or multimodal. Polymer decomposes.

[f] Polymer bi- or multimodal.

[g] Polymer insoluble in 1,2,4-trichlorobenzene.

Table 3
Copolymerization of ethene and norbornene at different comonomer ratios using catalyst **3**

Conditions[a]				Results			
x_{N}[b] (°C)	c_{mon}[c] ($\mathrm{mol\,l^{-1}}$)	n_{Pd} (μmol)	t_{pol} (h)	Activity[d]	T_{g} (°C)	M_{w} ($\mathrm{g\,mol^{-1}}$)	$M_{\mathrm{w}}/M_{\mathrm{n}}$
0.00	0.71	33.47	1.0	21	−43	7400	1.7
0.05	0.75	27.76	1.0	27	−1	21,000	1.8
0.10	0.80	26.88	1.0	36	44	51,000	1.8
0.20	0.89	26.88	1.0	55	83	111,000	1.9
0.25	0.95	13.39	1.0	84	91	140,000	1.7
0.30	1.02	26.69	1.0	70	104	167,000	1.3
0.34	1.08	26.69	1.0	83	108	162,000	1.8
0.40	1.19	26.69	1.0	83	123	161,000	1.8
0.50	1.18	19.94	1.0	79	125	168,000	1.8
0.60	1.16	26.69	1.0	71	136	191,000	1.6
0.80	1.03	33.36	1.0	26	151	94,000	1.7 [e]
1.00	2.37	33.47	1.5	36	[f]	[g]	[g]

Results of polymerizations at 30 °C in toluene.

[a] Total reaction volume 400 ml (norbornene homopolymerization: 100 ml).

[b] Mole fraction of norbornene in the feed.

[c] Total monomer concentration.

[d] Activity: $\mathrm{kg_{pol}\,mol_{Pd}^{-1}\,h^{-1}}$.

[e] Polymer bi- or multimodal. Polymer bi- or multimodal.

[f] Polymer decomposes.

[g] Polymer insoluble in 1,2,4-trichlorobenzene.

Mole fractions of norbornene in the feed of more than $x_{\mathrm{N}}=0.60$ do not lead to an increase in the incorporation level. Polymers produced under these conditions cannot be characterized faultlessly by means of ^{13}C NMR spectroscopy, due to the drastic broadening of the signals. Partially insoluble polymers are formed, that contain at least to some extend polynorbornene. Only catalyst **2** produced a polymer at $x_{\mathrm{N}}=0.80$ that could be investigated by ^{13}C NMR spectroscopy and even in this case no further increase in the norbornene content was observed.

3.1.2. Microstructures

Despite the complexity of the ^{13}C NMR spectra of ethene/norbornene copolymers, an almost complete assignment of the signals was achieved over the past years mainly by Arndt-Rosenau et al. [41,43], Fink et al. [44–48] and Tritto et al. [49–53], as well as others research groups [54–56]. All assignments were performed using copolymers made by group IV metallocene and constraint geometry catalysts. In conformity with results by Benedikt et al. [57] it is possible to apply these assignments also for products synthesized by late transition metals catalysts.

Table 4
Copolymerization of ethene and norbornene at different comonomer ratios using catalyst **4**

Conditions[a]				Results			
x_{N}[b] (°C)	c_{mon}[c] ($\mathrm{mol\,l^{-1}}$)	n_{Pd} (μmol)	t_{pol} (h)	Activity[d]	T_{g} (°C)	M_{w} ($\mathrm{g\,mol^{-1}}$)	$M_{\mathrm{w}}/M_{\mathrm{n}}$
0.00	0.73	23.14	2.0	40	−64	17,000	1.8
0.05	0.76	12.01	1.0	57	−29	27,000	1.8
0.10	0.81	24.03	1.0	57	10	52,000	1.7
0.20	0.90	24.03	1.0	65	53	66,000	2.0
0.25	0.96	23.61	1.0	74	65	87,000	1.5
0.30	1.03	23.61	1.0	68	81	93,000	1.4
0.35	1.08	24.44	1.0	66	88	109,000	1.6
0.40	1.19	24.03	1.0	62	98	159,000	1.2
0.50	1.19	23.14	1.0	56	100	145,000	2.1
0.59	1.17	24.44	1.0	36	104	71,000	1.7
0.80	0.85	21.84	1.0	7	[e]	[f]	[f]
1.00	2.37	27.30	120	[g]	[g]	[g]	[g]

Results of polymerizations at 30 °C in toluene.

[a] Total reaction volume 400 ml (norbornene homopolymerization: 100 ml).

[b] Mole fraction of norbornene in the feed.

[c] Total monomer concentration.

[d] Activity: $\mathrm{kg_{pol}\,mol_{Pd}^{-1}\,h^{-1}}$.

[e] Polymer bi- or multimodal. Polymer decomposes.

[f] Polymer insoluble in 1,2,4-trichlorobenzene.

[g] Catalyst inactive under these conditions.

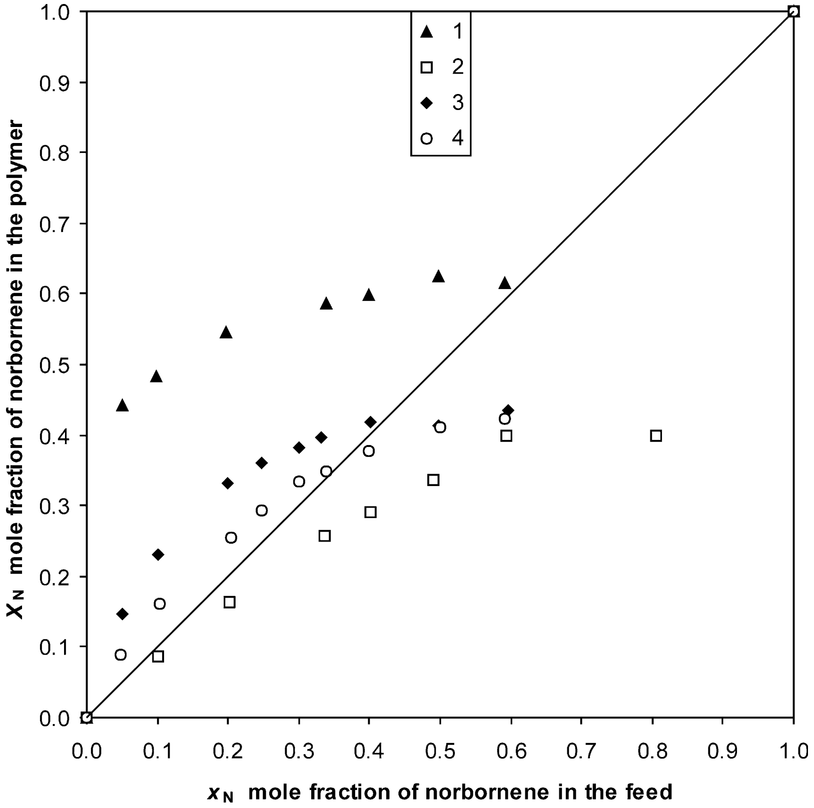

Fig. 2. Copolymerization diagrams. Copolymerization of ethene with norbornene performed by the catalysts **1**–**4** at 30 °C in toluene.

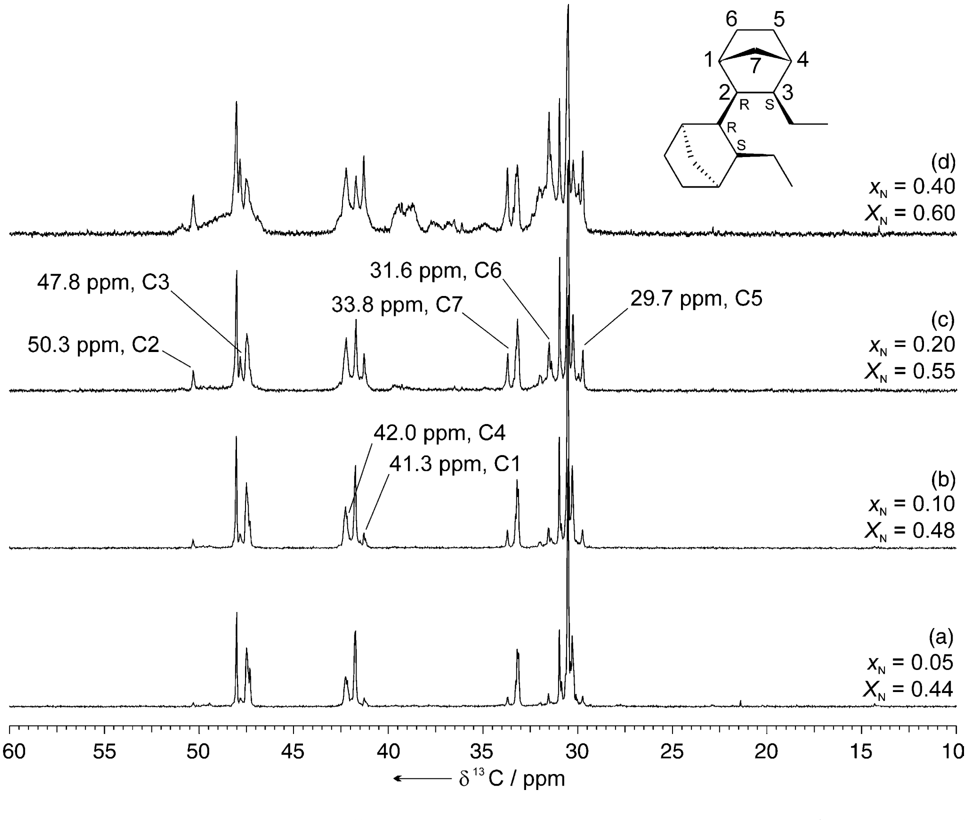

Fig. 3. ^{13}C NMR spectra of ethene/norbornene copolymers with different norbornene incorporations prepared by catalyst **1**. Assignments of chosen signals to carbon atoms of *rac*-norbornene diblock structures.

Fig. 3 shows ^{13}C NMR spectra of a series of ethene/norbornene copolymers with different norbornene fractions in the polymer prepared using catalyst **1**.

All copolymers produced by catalyst **1** show resonances of *rac*-connected norbornene diblock structures. The chemical shifts of the marked peaks are almost identical with resonances observed by Arndt-Rosenau [43] for metallocene/MAO catalyzed copolymers. Resonances that identify *meso*-connected norbornene diblocks (49.4, 42.7, 33.5, 32.0, 28.5 ppm for C2, C3, C1, C4, C7, C6, and C5 [43]) were not detected in any polymer. The exclusive observation of *rac*-norbornene diblocks indicates that the incorporation of norbornene follows a chain end control mechanism, since the achiral coordination site of **1** allows no influence on the molecular orientation during insertion. As expected, the signal areas of *rac*-norbornene diblock resonances increase with the norbornene incorporation.

Surprisingly, no discrete resonances are observed in regions that would clearly identify norbornene triblock structures (56.0–51.5 , 47.0–43.0 , 29.5–28.0 ppm) [46,48]. The sterical interaction of the ligand framework and the bulky polymer chain after the insertion of two consecutive norbornene units strongly favors the insertion of ethene as the next monomer. As a consequence, no norbornene mole fractions in the polymer higher than $X_N = 0.62$ are detected. At very high norbornene concentrations, a partial displacement of the neutral α-diimine against norbornene is possible which would lead to the formation of in-reactor blends of norbornene homo- and copolymers [35]. The vast increase in signal line width and the increasing insolubility of products formed under these conditions might be attributed to this displacement.

Fig. 4 shows a series of ^{13}C NMR spectra of ethene/norbornene copolymers made by catalyst **2**.

The ligand in **2** carries bulky isopropyl ortho substituents and a voluminous butane diimine bridge. The crowded coordination site is blocked already after the insertion of one norbornene unit in a way that only ethene insertion is possible. Almost no norbornene block structures are detectable even if norbornene-rich feed compositions are applied (Fig. 4(d)). As a consequence, mole fractions of norbornene in the polymer higher than $X_N = 0.50$ are not observed. Resonances of alternating structures are dominant (48.00 and 47.45 ppm for C2/C3; 42.16 and 41.71 ppm for C1/C4; 33.20 and 33.13 ppm for C7; 30.53 ppm for C5/C6) [43,53]. The polymers are practically atactic with only a slight excess of the syndiotactic alternating sequences.

The fraction of alternating structures decreases as the amount of norbornene in the feed is lowered and resonances of isolated norbornene units become dominant (Fig. 4(a): 47.29 ppm for C2/C3; 41.74 ppm for C1/C4; 33.07 ppm for C7; 30.49 ppm for C5/C6). Palladium based catalysts are known to undergo chain isomerization reactions between two insertion steps (chain walking) [18]. At norbornene poor conditions, signals typical for branched ethene sequences are, therefore, observed together with the norbornene resonances. A comparison with results published by Galland et al. [58] about the structure of branched polyethenes synthesized using Ni(II) α-diimine catalysts shows that methyl (19.95 ppm), ethyl (11.18 ppm), propyl (14.63 ppm), as well as butyl and longer branches (14.10 ppm) are formed. The resonances of branching points and methylene carbon atoms in branches overlap with norbornene signals of C5/C6 and C7. At higher norbornene fractions in the feed the vacant coordination site necessary for

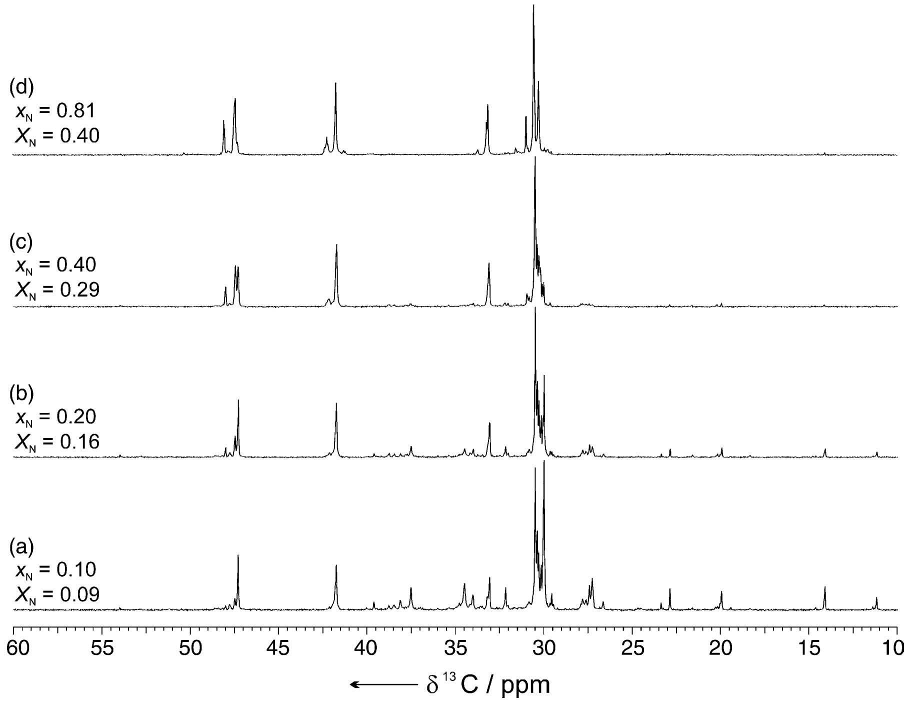

Fig. 4. ^{13}C NMR spectra of ethene/norbornene copolymers with different norbornene incorporations prepared by catalyst **2**.

the chain walking process is blocked by norbornene and the intensity of branching signals decreases.

The microstructures of copolymers produced by catalyst **4** are almost identical with the ones produced by **2**. Again alternating structures and sequences with isolated norbornene units are dominant. Differences result from the higher level of norbornene incorporation. The signal areas of branched ethene sequences are smaller. Resonances of norbornene diblock structures were detected for copolymers produced using norbornene rich feed compositions though the amount is still much lower than with catalyst **1**. These diblock structures are again exclusively *rac*-connected. Catalyst **3** carries only one ortho substituent which leads to a *trans* and *cis* isomer, formed in a 9:1 ratio during synthesis. The polymerization should, therefore, be performed mainly by the *trans* isomer. However, no influence of the chiral nature of the coordination site was observed and the microstructures are similar to the ones of copolymers produced with **2** and **4**. In conformity with the higher norbornene content, the amount of *rac*-norbornene diblocks is again higher than with catalyst **4**.

3.1.3. Catalytic activities and turnover frequencies

Tempel et al. investigated the influence of the ligand structure on the migratory insertion rate of the (α-diimine)Pd(II) catalyzed ethene polymerization using low temperature ^{1}H NMR spectroscopic measurements of model compounds [39]. Increased sterical bulk of the *ortho*- *N*-aryl substituents and of the bridge unit was assumed to raise the ground-state energy of the corresponding alkyl ethene complex, resulting in a lower activation barrier for the migratory insertion. If these results are transferred to the copolymerization of ethene and norbornene it has to be considered that palladium based complexes show a preference for the coordination of the electron richer and softer monomer norbornene. On the other hand, norbornene coordination is complicated by the sterical interactions between the α-diimine ligand and bulky monomer.

For the comparison of the catalysts it is advantageous to use the turnover frequency (TOF), i.e. the number of moles of monomers converted to polymer per mole of catalyst (n_{Pd}) per unit of time (t_{pol}), instead of the activities as listed in the Tables 1–4. The activities do not consider the different norbornene incorporation levels of the individual polymers. Since the molar mass of norbornene ($M_{\mathrm{N}}=94.16\ \mathrm{g\ mol}^{-1}$) is somewhat higher than of ethene ($M_{\mathrm{E}}=28.05\ \mathrm{g\ mol}^{-1}$), a norbornene rich copolymer will always show a higher activity than an ethene rich polymer even if the rate of insertions is equal. The use of TOF's, calculated from the polymer yield m_{pol} and the weight fraction of norbornene in the polymer W_{N} using Eq. (1), avoids this problem.

$$\mathrm{TOF} = \frac{\left[\frac{m_{\mathrm{pol}} W_{\mathrm{N}}}{M_{\mathrm{N}}}\right] + \left[\frac{m_{\mathrm{pol}}(1-W_{\mathrm{N}})}{M_{\mathrm{E}}}\right]}{n_{\mathrm{PD}} t_{\mathrm{pol}}} \tag{1}$$

Fig. 5 shows the TOF's as a function of the mole fraction of norbornene in the feed.

Consistent with the results by Tempel et al., catalyst **2** shows the highest overall insertion rate in the homopolymerization of ethene. If norbornene is added to the reaction mixture, the insertion rate decreases since the active site is blocked already

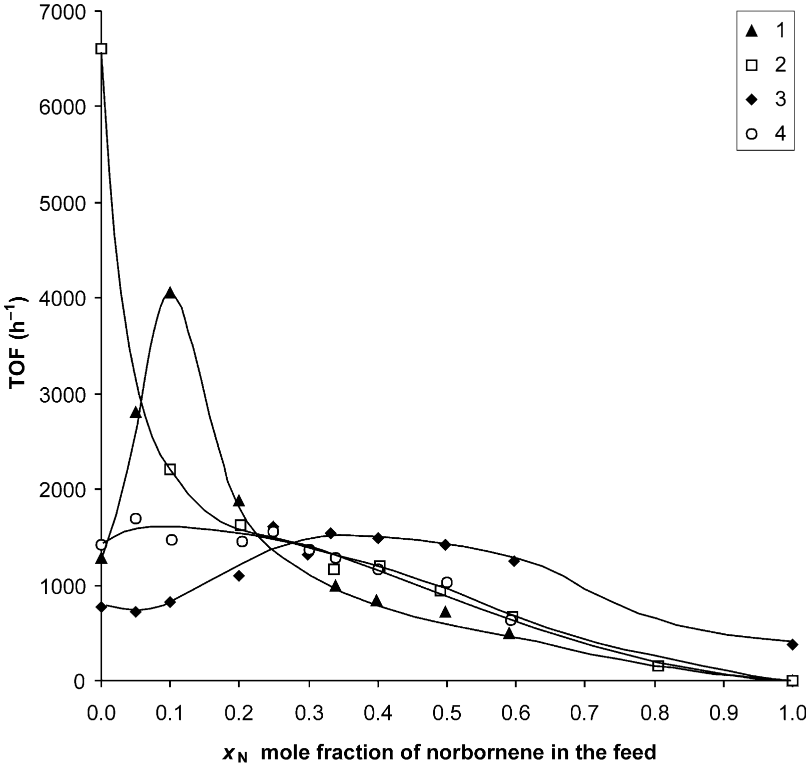

Fig. 5. Turnover frequencies TOF as a function of the mole fraction of norbornene in the polymer X_{N}. Ethene norbornene copolymerizations using catalysts **1**–**4** at 30 °C in toluene.

after one norbornene insertion and only ethene can be inserted as the next monomer. The smaller ethene concentration at increasing mole fractions of norbornene causes a further reduction of the insertion rate.

Compared to **2**, catalyst **1** shows a much lower TOF in the ethene homopolymerization. The relative open structure of the active site allows facile norbornene coordination and insertion and the polymerization rate is increasing rapidly. Norbornene diblock structures are formed instantly. At norbornene fractions in the feed higher than $x_N = 0.10$, catalyst **1** shows the same decrease in the TOF's like **2**, due to the blockage of the active site after two consecutive norbornene insertions.

The catalysts **3** and **4** again show a behavior between the extremes of **1** und **2**. The catalytic performance of **4** resembles the one of **2**, yet without the high insertion rates in ethene homopolymerization. At norbornene rich feed compositions between $x_N = 0.3$ and 0.6, **3** shows the highest TOF's of all catalysts. Like in **1**, the active site allows facile norbornene coordination, due to the presence of only one though bulky ortho substituent at the *N*-aryl ring. In addition, **3** is the only catalyst that is active in the homopolymerization of norbornene. This behavior is assumed to result from catalyst decomposition reactions and, therefore, the presence of 'naked' palladium in the reaction mixture.

3.1.4. Molar masses and polydispersities

In order to obtain high molar mass polymers, the rate of chain transfer reactions has to be reduced relative to the rate of chain propagation. According to combined DFT and molecular mechanic calculations by Ziegler et al. for the ethene polymerization with Ni(II) α-diimines [59,60], chain transfer proceeds in a concerted process in which a β-hydrogen is directly transferred to the coordinated monomer without an olefin hydride intermediate. The transition state in this process occupies both axial positions of the square planar complex. Bulky ortho substituents and rigid bridge units force the *N*-aryl rings to project in an axial position of the metal center and, therefore, complicate chain transfer. The transition state of the migratory insertion only occupies the equatorial coordination sides and is, therefore, far less affected by the ortho substituents.

The weight averages of the molar masses are listed in Tables 1–4. The ethene homopolymers produced by catalysts **1–4** are in conformity with these investigations, but some deviations are observed when norbornene is added to the reaction mixture. As expected, catalyst **1** produces copolymers with the lowest molar mass and the highest norbornene contents. When regarding low norbornene incorporation levels, catalyst **2** produces the highest molecular weights. Surprisingly, catalyst **3** and **4** produce copolymers with comparatively high norbornene contents together with high molar masses. Catalyst **4** was expected to show a behavior comparable to that of catalyst **2**.

Most of the polymers produced by the catalysts **1–4** are monomodal. Bi- or multimodal polymers are observed if high norbornene fractions in the feed of more than $x_N = 0.60$ are applied. Again this can be attributed to a partial ligand displacement and, therefore, the generation of different active

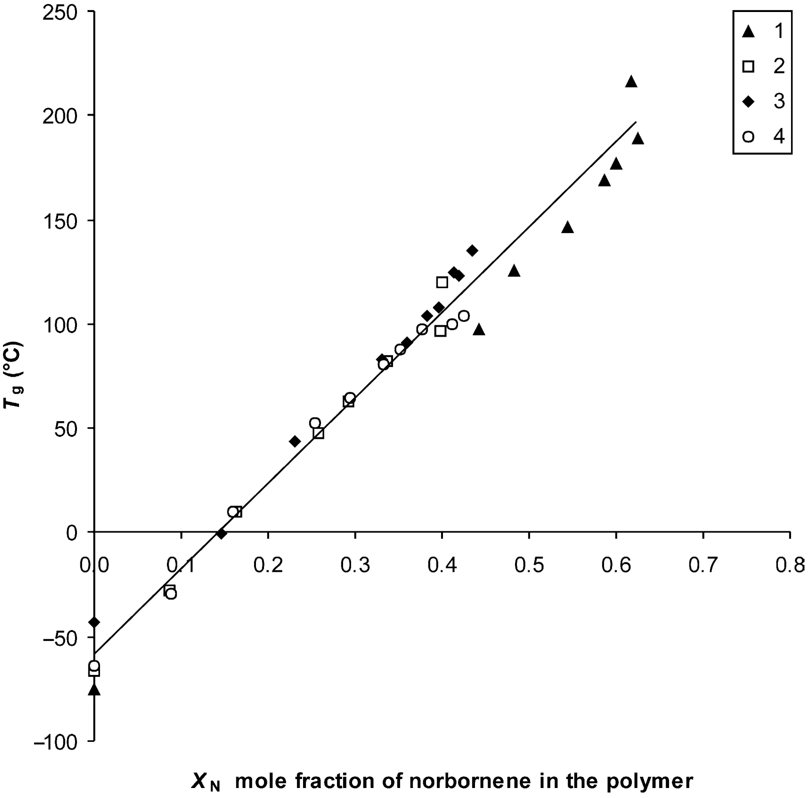

Fig. 6. Glass transition temperatures T_g as a function of the mole fraction of norbornene in the polymer X_N. Ethene norbornene copolymerizations using catalysts **1–4** at 30 °C in toluene.

sites. The polydispersities M_w/M_n of monomodal copolymers are generally lower than **2**. Although the observed values are low compared to group IV metallocene/methylaluminoxane catalysts, chain transfer is assumed to be significant under the chosen conditions. This behavior is in accordance with results found by Brookhart et al. on the living homopolymerization of ethene and α-olefins with palladium(II) [61] and nickel(II) α-diimines [62], respectively. Some of the bi- or multimodal polymers show polydispersities under $M_w/M_n = 2$ since the component peaks in the GPC curve show very narrow distributions.

3.1.5. Glass transition temperature

The glass transition temperature T_g is closely related to the norbornene contend of the polymer.

Fig. 6 shows a linear dependence of the T_gs on the norbornene content of the copolymers in accordance with various results reported in literature [40–42,54]. At low norbornene incorporation levels, deviations from a linear relationship are caused by the presence of branched structures along the methylene sequences [63]. Norbornene block structures lead to an increased stiffness of the polymer backbone and, therefore, higher T_g [55,64,65]. Considering the copolymers investigated in this study, these influences cause minor deviations. Only the copolymers produced by catalyst **1** show slightly lower glass transition temperatures than expected, even though they contain larger amounts of norbornene diblocks. This fact can be attributed to the generally lower molecular masses of the copolymers. Melting points were not observed in any thermogram [66].

3.2. Effect of the polymerization temperature

The influence of the polymerization temperature on the catalyst activity and the properties of the resultant copolymers was investigated. For this purpose, copolymerizations were performed at −20, −10, 0, 10, 15, 20, 30, 45, and 60 °C at a fixed feed composition of $x_N = 0.33$ with all of the catalyst. In addition, catalyst **1** was used in temperature experiments at a fixed norbornene fraction in the feed of $x_N = 0.10$, where it showed its highest activity (Fig. 5). The reaction conditions were again chosen to keep the norbornene conversion low and at the same time yield sufficient polymer for characterization. They are summarized together with the results in Tables 5–9.

3.2.1. Norbornene incorporation and glass transition temperatures

If catalyst carrying bulky isopropyl ligands are applied (**2** and **4**), the mole fraction of norbornene in the polymer decreases constantly as the polymerization temperature is raised. The effect is more distinct for catalyst **4**. In case of catalysts **1**, bearing a less blocked coordination site, the norbornene incorporation level reaches a maximum at 0 °C ($x_N = 0.10$) and at 30 °C ($x_N = 0.33$), respectively. As expected, the overall incorporation level is lower at a feed composition of $x_N = 0.10$. At polymerization temperatures below 0 °C, the incorporation level decreases rapidly. As a consequence of this different behavior, at −20 °C catalyst **4** produces polymers that exhibit the same norbornene incorporation as catalyst **1**. At low temperatures, catalyst **3** shows a behavior comparable to that of catalyst **1**, whereas at temperatures above 10 °C the norbornene incorporation is more or less constant.

Similar trends are observed for the dependence of the glass transition temperature on the polymerization temperature. This behavior confirms the linear relation of the norbornene incorporation and the glass transition temperatures. Again deviations are mainly based on differences in the molar masses of the copolymers.

The microstructures are influenced by the polymerization temperature only due to the different norbornene incorporation level. Copolymers that are produced by the same catalyst and that contain the same mole fraction of norbornene show identical ^{13}C NMR spectra even if they produced at different temperatures.

Table 5
Copolymerization of ethene with norbornene at different polymerization temperatures using catalyst **1**

Conditions[a]				Results				
T_{pol} (°C)	c_{mon}[b] (mol l^{-1})	n_{Pd} (μmol)	t_{pol} (h)	Activity[c]	X_N[d]	T_g (°C)	M_w (g mol^{-1})	M_w/M_n
−20	2.17	9.77	5.00	16	0.46	134	91,000	1.1
−10	1.71	4.87	3.75	29	0.50	136	123,000	1.3
0	1.37	4.87	2.50	65	0.52	135	127,000	1.6
10	1.12	3.91	0.75	131	0.49	135	98,000	1.7
15	1.05	4.87	0.75	208	0.50	132	79,000	1.8
20	0.94	4.87	0.75	239	0.50	129	67,000	1.7
30	0.80	4.19	1.00	243	0.48	126	39,000	2.0
45	0.64	4.87	0.75	84	0.46	112	21,000	1.9
60	0.55	4.87	0.75	39	0.38	100	18,000	1.9[e]

Results of polymerizations at $x_N = 0.10$ in toluene.

[a] Total reaction volume 400 ml.

[b] Total monomer concentration.

[c] Activity: $kg_{pol}\ mol_{Pd}^{-1}\ h^{-1}$.

[d] Mole fraction of norbornene in the polymer.

[e] Polymer bi- or multimodal.

Table 6
Copolymerization of ethene with norbornene at different polymerization temperatures using catalyst **1**

Conditions[a]				Results				
T_{pol} (°C)	c_{mon}[b] (mol l^{-1})	n_{Pd} (μmol)	t_{pol} (h)	Activity[c]	X_N[d]	T_g (°C)	M_w (g mol^{-1})	M_w/M_n
−20	1.25	7.73	4.00	13	0.45	155	65,000	1.1
−10	1.05	4.29	3.00	34	0.51	155	113,000	1.2
0	1.17	4.29	3.00	93	0.55	166	213,000	1.5
10	1.07	3.91	2.00	158	0.55	168	173,000	1.8
15	1.14	4.29	1.00	262	0.56	167	175,000	1.8
20	1.27	3.91	1.00	228	0.58	172	151,000	2.0
30	0.71	8.38	1.00	67	0.59	169	66,000	1.8
45	0.87	3.87	0.50	61	0.50	153	38,000	1.9[e]
60	0.74	4.29	0.50	27	0.39	140	19,000	1.6[e]

Results of polymerizations at $x_N = 0.33$ in toluene.

[a] Total reaction volume 400 ml.

[b] Total monomer concentration.

[c] Activity: $kg_{pol}\ mol_{Pd}^{-1}\ h^{-1}$.

[d] Mole fraction of norbornene in the polymer.

[e] Polymer bi- or multimodal.

3.2.2. Activities and turnover frequencies

All catalysts show maximum TOF's at temperatures between 15 and 30 °C. The polymerization rate is reduced significantly when lower polymerization temperatures are applied. Longer polymerization times are required in order to yield sufficient polymer for characterization. Under these conditions, an almost constant consumption of ethene is observed during the course of the reaction. Fast decomposition of the catalysts is observed at temperatures above 30 °C, usually within 15–30 min. As expected, catalyst **1** shows the highest overall incorporation rate. The sharp maximum at 15 °C is shifted to a broader maximum at 30 °C when the amount of norbornene in the feed is reduced from $x_N = 0.33$ to 0.10. This result indicates that higher norbornene concentrations play a key role in catalyst decomposition. A similar dependence on the polymerization temperature is observed for catalyst **2**, though on a generally lower level. The maximum activity is observed at 20 °C. Catalysts **3** and **4** show an almost identical behavior with broader maxima at 30 °C.

3.2.3. Molar masses and polydispersities

As expected, the molar masses decrease strongly when the polymerization temperature surpasses 30 °C. At elevated temperatures, differences in the activation energies of chain termination reactions and chain propagation reactions are of decreasing importance, leading to lower molar masses. This trend is intensified by the progressing decay of the catalysts. Polymers produced at temperatures above 30 °C are often bi- or multimodal. Nevertheless, the overall polydispersities of these polymers are again low with values around or under $M_w/M_n = 2$ due to the very narrow distribution of the individual component peaks. The molar masses decrease also at low temperatures mainly due to the significantly lower polymerization rate. Catalyst **1**, which showed the highest activities over the whole temperature area, produced the highest molar mass polymers at 0 °C independent of the mole fraction of norbornene in the feed. The maximum is shifted to higher temperatures for the other, less active catalysts (20 °C for **2**, 30 °C for **3** and **4**).

Table 7
Copolymerization of ethene with norbornene at different polymerization temperatures using catalyst **2**

Conditions[a]				Results				
T_{pol} (°C)	c_{mon}[b] (mol l^{-1})	n_{Pd} (μmol)	t_{pol} (h)	Activity[c]	X_N[d]	T_g (°C)	M_w (g mol^{-1})	M_w/M_n
−20	1.26	15.55	4.0	5	0.31	97	52,000	1.8
−10	1.42	15.55	3.0	7	0.30	79	25,000	1.1
0	1.52	7.75	3.0	21	0.31	72	69,000	1.2
10	1.56	7.75	1.0	68	0.28	67	128,000	1.2
15	1.05	7.79	1.0	79	0.28	61	110,000	1.2
20	1.28	7.75	1.0	106	0.29	58	131,000	1.5
30	0.71	7.77	1.0	53	0.26	48	106,000	1.7
45	0.87	7.75	1.0	28	0.26	45	63,000	1.8
60	0.74	7.75	0.5	24	0.23	34	36,000	1.6[e]

Results of polymerizations at $x_N = 0.33$ in toluene.

[a] Total reaction volume 200 ml.

[b] Total monomer concentration.

[c] Activity: $kg_{pol}\ mol_{Pd}^{-1}\ h^{-1}$.

[d] Mole fraction of norbornene in the polymer.

[e] Polymer bi- or multimodal.

Table 8
Copolymerization of ethene with norbornene at different polymerization temperatures using catalyst **3**

Conditions[a]				Results				
T_{pol} (°C)	c_{mon}[b] (mol l^{-1})	n_{Pd} (μmol)	t_{pol} (h)	Activity[c]	X_N[d]	T_g (°C)	M_w (g mol^{-1})	M_w/M_n
−20	1.27	16.59	5.0	5	0.31	104	39,000	1.4
−10	0.96	17.54	3.0	9	0.33	115	40,000	1.3
0	0.87	26.78	2.0	14	0.37	114	62,000	1.5
10	1.14	6.18	2.0	38	0.42	119	100,000	1.5
15	0.87	26.78	1.0	49	0.40	107	101,000	1.5
20	0.83	8.30	1.0	61	0.42	110	106,000	1.7
30	1.08	26.69	1.0	83	0.40	108	162,000	1.8
45	0.86	17.54	1.0	28	0.41	105	103,000	2.0[e]
60	0.74	26.78	1.0	12	0.38	103	46,000	1.5[e]

Results of polymerizations at $x_N=0.33$ in toluene.
[a] Total reaction volume 400 ml.
[b] Total monomer concentration.
[c] Activity: $kg_{pol}\ mol_{Pd}^{-1}\ h^{-1}$.
[d] Mole fraction of norbornene in the polymer.
[e] Polymer bi- or multimodal.

According to the results published by Brookhart et al. [61] on the living polymerization of ethene with palladium α-diimine catalysts, a constant decrease in the polydispersities is expected at decreasing polymerization temperatures. The investigated catalysts generally follow this trend though some deviations are observed.

4. Summary and conclusions

The investigated cationic palladium α-diimine complexes are efficient catalysts for the copolymerization of ethene and norbornene. It is possible to deduce relations between the steric demand of the α-diimine ligand and the properties of the resulting copolymers. The incorporation of norbornene in the polymer is usually very high with up to $X_N=0.62$ and adjustable by choice of the catalyst and appropriate polymerization conditions. The high glass transition temperatures correspond to these high norbornene contents. Copolymers with low mole fractions of norbornene show alternating microstructures or isolated norbornene units along the polymer chain. If the incorporation level exceeds $X_N=0.45$, *racemic* connected norbornene diblock structures are observed. The formation of block structures is chain end controlled while alternating structures are practically atactic. Higher norbornene blocks are not identified. Molar masses of the copolymers range from oligomeric levels to high polymers. When norbornene fractions in the feed of more than $x_N=0.60$ are applied, partially or totally insoluble polymers are formed. This observation is assumed to originate in a partial ligand displacement through norbornene and, therefore, the formation of polynorbornene. Polymers produced under these conditions are bi- or multimodal. The polydispersities of monomodal copolymers are generally below 2.

The catalysts deactivate rapidly at polymerization temperatures above 30 °C. In addition, the incorporation of norbornene and the molar masses decreases. Polymerization temperatures below 10 °C result in a reduction of the polymerization rate and the molar masses. The low temperature behavior concerning the norbornene incorporation differs for the investigated catalysts. Catalysts that carry bulky isopropyl *ortho*-

Table 9
Copolymerization of ethene with norbornene at different polymerization temperatures using catalyst **4**

Conditions[a]				Results				
T_{pol} (°C)	c_{mon}[b] (mol l^{-1})	n_{Pd} (μmol)	t_{pol} (h)	Activity[c]	X_N[d]	T_g (°C)	M_w (g mol^{-1})	M_w/M_n
−20	1.54	33.11	5.0	3	0.43	118	26,000	1.3
−10	1.26	33.11	4.0	5	0.43	112	41,000	1.4
0	1.01	23.11	2.1	16	0.41	104	56,000	1.5
10	0.86	22.49	1.0	36	0.39	101	83,000	1.2
15	0.86	22.49	1.0	48	0.36	94	92,000	1.4
20	0.86	22.49	1.0	59	0.36	90	74,000	1.3
30	1.08	24.44	1.0	66	0.35	88	110,000	1.6
45	0.86	22.49	1.0	29	0.32	77	47,000	1.7[e]
60	0.72	21.85	1.0	12	0.27	62	24,000	1.5[e]

Results of polymerizations at $x_N=0.33$ in toluene.
[a] Total reaction volume 400 ml.
[b] Total monomer concentration.
[c] Activity: $kg_{pol}\ mol_{Pd}^{-1}\ h^{-1}$.
[d] Mole fraction of norbornene in the polymer.
[e] Polymer bi- or multimodal.

substituents show a constant decrease in the norbornene content as the polymerization temperature is raised, while a maximum incorporation is observed between 0 and 30 °C for the other catalysts.

References

[1] Lamonte RR, McNally D. Adv Mater Process 2001;159:33–6.
[2] Sparenberg B. Kunststoffe 2004;94:134–7.
[3] Anderson AW, Merckling NG. (EI du Pont de Nemours) US Patent 2721189; 1955 [Chem Abstr 1956;50:14596].
[4] Natta G, Pasquon I, Zambelli A, Giustiniani PA. (Montecatini) BE Patent 616851; 1962 [Chem Abstr 1963;58:15167].
[5] Koinzer JP, Langbein U, Taeger E. (VEB Leuna-Werke) DE Patent 2421838; 1975 [Chem Abstr 1976;84:60227].
[6] Lindner R, Wurbs A, Koinzer JP, Geyer W, Grahlert W, Langbein U, et al. (VEB Leuna-Werke) DD Patent 222317; 1985 [Chem Abstr 1985;103:215969].
[7] Kaminsky W, Bark A, Arndt M. Makromol Chem Macromol Symp 1991; 47:83–93.
[8] Kaminsky W, Arndt M, Bark A. Polym Prepr (Am Chem Soc Div Polym Chem) 1991;32:467–8.
[9] Kaminsky W, Bark A, Steiger R. J Mol Catal 1992;74:109–19.
[10] Kaminsky W, Noll A. Polym Bull 1993;31:175–82.
[11] Glockner PW, Keim W, Mason RF, Bauer RS. (Shell Internationale Research Maatschappij) DE Patent 2053758; 1971 [Chem Abstr 1971;75:88072].
[12] Keim W, Kowaldt FH, Goddard R, Krüger C. Angew Chem, Int Ed Engl 1978;17:466–7.
[13] Peuckart M, Keim W. Organometallics 1983;2:594–7.
[14] Ostoja-Starzewski KHA, Witte J. Angew Chem, Int Ed Engl 1985;24: 599–601.
[15] Ostoja-Starzewski KHA, Witte J. Angew Chem, Int Ed Engl 1987;26: 63–4.
[16] Klabunde U, Mülhaupt R, Herskovitch T, Janowicz A, Calabrese H, Ittel SD. J Polym Sci, Part A: Polym Chem 1987;25:1989–2003.
[17] Klabunde U, Ittel SD. J Mol Catal 1987;41:123–4.
[18] Johnson LK, Killian CM, Brookhart M. J Am Chem Soc 1995;117: 6414–5.
[19] Johnson LK, Killian CM, Arthur SD, Feldman J, McCord EF, McLain SJ, et al. (University of North Carolina, Chapel Hill/EI DuPont de Nemours), WO Patent 9623010; 1996 [Chem Abstr 1996;125:222773t].
[20] Gates DP, Svejda SA, Oñate E, Killian CM, Johnson LK, White PS, et al. Macromolecules 2000;33:2320–34.
[21] Svoboda M, Tom Dieck H. J Organomet Chem 1980;191:321–8.
[22] Tom Dieck H, Svoboda M, Greiser T. Z Naturforsch 1981;36b:823–32.
[23] van Koten G, Vrieze K. Adv Organomet Chem 1982;21:151–239.
[24] van Asselt R, Elsevier CJ, Smeets WJJ, Spek AL, Benedix R. Recl Trav Chim Pays-Bas 1994;113:88–98.
[25] van Asselt R, Gielens EECG, Ruelke R, Vrieze K, Elsevier CJ. J Am Chem Soc 1994;116:977–85.
[26] Johnson LK, Mecking S, Brookhart M. J Am Chem Soc 1996;118:267–8.
[27] Mecking S, Johnson LK, Wang L, Brookhart M. J Am Chem Soc 1998; 120:888–99.
[28] Fernandes S, Marques MM, Correia SG, Mano J, Chien JCW. Macromol Chem Phys 2000;201:2566–72.
[29] Held A, Mecking S. Chem Eur J 2000;6:4623–9.
[30] Bauers FM, Mecking S. Macromolecules 2001;34:1165–71.
[31] Soula R, Novat C, Tomov A, Spitz R, Claverie J, Drujon X, et al. Macromolecules 2001;34:2022–6.
[32] Soula R, Saillard B, Spitz R, Claverie J, Llaurro MF, Monnet C. Macromolecules 2002;35:1513–23.
[33] Mecking S, Held A, Bauers FM. Angew Chem, Int Ed Engl 2002;41: 544–61.
[34] Makovetsky KL, Finkelstein ES, Bykov VI, Bagdasaryan AK, Goodall BL, Rhodes LF. (The BF Goodrich Company) WO Patent 9856837; 1998 [Chem Abstr 1999;130:66910].
[35] Goodall BL, McIntosh LH. (The BF Goodrich Company). WO Patent 9856839; 1998 [Chem Abstr 1999;130:66911].
[36] Kiesewetter J, Kaminsky W. Chem Eur J 2003;9:1750–8.
[37] Rülke RE, Ernsting JM, Spek AL, Elsevier CJ, van Leeuwen PWNM, Vrieze K. Inorg Chem 1993;32:5769–78.
[38] Brookhart M, Grant B, Volpe Jr AF. Organometallics 1992;11:3920–2.
[39] Tempel DJ, Johnson LK, Huff RL, White PS, Brookhart M. J Am Chem Soc 2000;122:6686–700.
[40] Ruchatz D, Fink G. Macromolecules 1998;31:4681–3.
[41] Arndt M, Beulich I. Macromol Chem Phys 1998;199:1221–32.
[42] Cherdron H, Brekner MJ, Osan F. Angew Makromol Chem 1994;223: 121–33.
[43] Arndt-Rosenau M, Beulich I. Macromolecules 1999;32:7335–43.
[44] Ruchatz D, Fink G. Macromolecules 1998;31:4674–80.
[45] Wendt RA, Mynott R, Hauschild K, Ruchatz D, Fink G. Macromol Chem Phys 1999;200:1340–50.
[46] Wendt RA, Fink G. Macromol Chem Phys 2001;202:3490–501.
[47] Wendt RA, Mynott R, Fink G. Macromol Chem Phys 2002;203:2531–9.
[48] Wendt RA, Fink G. J Mol Catal A: Chem 2003;203:101–11.
[49] Provasoli A, Ferro DR, Tritto I, Boggioni L. Macromolecules 1999;32: 6697–706.
[50] Tritto I, Marestin C, Boggioni L, Zetta L, Provasoli A, Ferro DR. Macromolecules 2000;33:8931–44.
[51] Tritto I, Marestin C, Boggioni L, Sacchi MC, Brintzinger HH, Ferro DR. Macromolecules 2001;34:5770–7.
[52] Tritto I, Boggioni L, Jansen JC, Thorshaug K, Sacchi MC, Ferro DR. Macromolecules 2002;35:616–23.
[53] Tritto I, Boggioni L, Ferro DR. Macromolecules 2004;37:9681–93.
[54] Rische T, Waddon AJ, Dickinson LC, MacKnight WJ. Macromolecules 1998;31:1871–4.
[55] Bergström CH, Sperlich BR, Ruotoistenmäki J, Seppälä JV. J Polym Sci, Part A: Polym Chem 1998;36:1633–8.
[56] McKnight AL, Waymouth RM. Macromolecules 1999;32:2816–25.
[57] Benedikt GM, Elce E, Goodall BL, Kalamarides HA, McIntosh III LH, Rhodes LF, et al. Macromolecules 2002;35:8978–88.
[58] Galland GB, de Souza RF, Mauler RS, Nunes FF. Macromolecules 1999; 32:1620–5.
[59] Deng L, Margl P, Ziegler T. J Am Chem Soc 1997;119:1094–100.
[60] Deng L, Woo TK, Cavallo L, Margl PM, Ziegler T. J Am Chem Soc 1997; 119:6177–86.
[61] Gottfried AC, Brookhart M. Macromolecules 2001;34:1140–2.
[62] Killian CM, Tempel DJ, Johnson LK, Brookhart M. J Am Chem Soc 1996;118:11664–5.
[63] Mäder D, Heinemann J, Walter P, Mülhaupt R. Macromolecules 2000;33: 1254–61.
[64] Bergström CH, Väänänen TLJ, Seppälä JV. J Appl Polym Sci 1997;63: 1071–6.
[65] Forsyth J, Pereña JM, Benavente R, Perez E, Tritto I, Boggioni L, et al. Macromol Chem Phys 2001;202:614–20.
[66] Harrington BA, Crowther DJ. J Mol Catal A: Chem 1998;128:79–84.